

**Nonpercolative metal-insulator transition in VO<sub>2</sub> single crystals**Bongjin Simon Mun,<sup>1</sup> Kai Chen,<sup>2,3</sup> Joonseok Yoon,<sup>4</sup> Catherine Dejoie,<sup>2</sup> Nobumichi Tamura,<sup>2</sup> Martin Kunz,<sup>2</sup> Zhi Liu,<sup>2</sup> Michael E. Grass,<sup>1,2</sup> Sung-Kwan Mo,<sup>2</sup> Changwoo Park,<sup>5</sup> Y. Yvette Lee,<sup>4</sup> and Honglyoul Ju<sup>4,\*</sup><sup>1</sup>*Department of Applied Physics, Hanyang University, Ansan, Kyunggi-Do 426-791, Republic of Korea*<sup>2</sup>*Advanced Light Source, Lawrence Berkeley National Laboratory, Berkeley, California 94720, USA*<sup>3</sup>*Center for Advancing Materials Performance from the Nanoscale (CAMP-Nano), State Key Laboratory for Mechanical Behavior of Materials, Xi'an Jiaotong University, Xi'an 710049, China*<sup>4</sup>*Department of Physics, Yonsei University, Seoul 120-749, Republic of Korea*<sup>5</sup>*Division of Applied Chemistry and Biotechnology, Hanbat National University, Daejeon 305-719 and Advanced Nano Products, Chungwon, Chungbuk 363-942, Republic of Korea*

(Received 11 August 2011; published 21 September 2011)

Detailed temperature-dependent transport, optical microscopy, and synchrotron-based polychromatic x-ray microdiffraction measurements have been carried out in the vicinity of the metal-insulator transition (MIT) temperature of VO<sub>2</sub> single crystals. The formation and propagation of a real-space phase boundary along the rutile *c* axis is monitored during the transition. Pure metallic rutile R, as well as insulating monoclinic M1 phases, is observed at the onset of MIT. The two phases are separated by a sharp-phase boundary. Our findings suggest a nonpercolative nature of the MIT in VO<sub>2</sub>.

DOI: [10.1103/PhysRevB.84.113109](https://doi.org/10.1103/PhysRevB.84.113109)

PACS number(s): 71.30.+h, 61.50.Ks, 71.27.+a

VO<sub>2</sub> is one of the most widely studied, strongly correlated electron materials because of its spectacular metal-insulator transition (MIT) near room temperature ( $\sim 67^\circ\text{C}$ ) and its complex interplay with the lattice.<sup>1-5</sup> Two mechanisms have been generally considered to explain the origin of the MIT in VO<sub>2</sub>. The Mott-Hubbard mechanism suggests that electron-electron correlation drives the first-order MIT,<sup>2,3</sup> whereas the Peierls mechanism proposes that a strong electron-lattice interaction leads to the MIT.<sup>4,5</sup> However, the simultaneous occurrence of a structural phase transition (SPT) makes it difficult to identify the exact mechanism.<sup>6</sup> For this reason intense research activity continues to try to elucidate whether a Peierls mechanism or a Mott-Hubbard mechanism is primary.

Recently, it is experimentally shown that both the electronic and structural transitions occur in a percolative manner near phase transition of VO<sub>2</sub>-thin films, i.e., the mixtures of both electronic and crystalline phases exist near MIT. With scanning near-field infrared microscopy<sup>6</sup> and nanoscale x-ray diffraction,<sup>7</sup> the presence of percolation behavior among the metallic nanoscale domains and local nonmonotonic lattice structures are found as temperature increases. Similarly, a percolation model is applied to explain the results of x-ray diffraction and scanning tunneling spectroscopy data of VO<sub>2</sub> films.<sup>8</sup> In the percolation model the effective transport property of a material is modeled with networks of nanoscale domains of different sizes near critical temperature.<sup>9</sup> The importance of this percolative behavior in VO<sub>2</sub> lies on the fact that a dichotomy between MIT and SPT exist in understanding phase transition of VO<sub>2</sub>. However, considering many past works in VO<sub>2</sub>, which support either the pictures of Mott-Hubbard model or Peierls model,<sup>2-4</sup> the presence of the dichotomy in VO<sub>2</sub> is somewhat surprising and brings out the question whether this is the true intrinsic property of VO<sub>2</sub>. As widely accepted, the influence of the interfacial strains or stress is difficult to overlook when the thin films of VO<sub>2</sub> prepared on foreign substrates are used for the measurement. In the study of strongly correlated materials the influence of the lattice

distortion has also become an important factor in understanding the configuration of spatially inhomogeneous phases under strong Coulomb interactions.<sup>10</sup> More importantly, whether the percolative scenarios can be applied to the bulk VO<sub>2</sub>, as in other correlated electron systems,<sup>11</sup> remains to be an open question. In the recent report of Sharoni *et al.*, the percolation model cannot fully explain the details of the transport characteristics of VO<sub>2</sub> at MIT.<sup>12</sup>

In this Brief Report we present transport, optical microscopy, and synchrotron-based x-ray microdiffraction data of VO<sub>2</sub> with unprecedented details of structures in the temperature dependence. Our data suggest the existence of sharp-phase boundary between metallic R and insulating M1 states. The MIT occurs through the propagation of the phase boundary along a particular crystal axis. Contrary to the percolative pictures on VO<sub>2</sub>-thin films, our finding provides an evidence of a nonpercolative characteristic in VO<sub>2</sub> single crystals.

VO<sub>2</sub> single crystals were prepared by the self-flux method; details of crystal growth can be found elsewhere.<sup>13</sup> The resistance of a VO<sub>2</sub> single crystal was measured as a function of temperature. The resistance was measured using a dc technique with the two-contact four-probe method. Indium metal was used as a contact material for the electrical measurement. Then the sample was mounted on a sapphire plate attached to copper heating block. In this experimental set-up we can assume that the gradient of the sample temperature was close to zero. Figure 1(a) shows the results of the resistance measurements indicating two phase transitions. The first transition occurs at  $49.7^\circ\text{C}$  during heating and  $46.4^\circ\text{C}$  during cooling, whereas the second transition is observed at  $67.2^\circ\text{C}$  during heating and  $62.2^\circ\text{C}$  during cooling. The first transition is an insulator-insulator structural phase transition (IIT) between two monoclinic phases, M2 (low temperature) and M1 (high temperature), which was previously reported based on  $\mu$ -XRD results.<sup>13</sup> At  $\sim 67.2^\circ\text{C}$ , the MIT is observed, as evidenced by a change in resistance

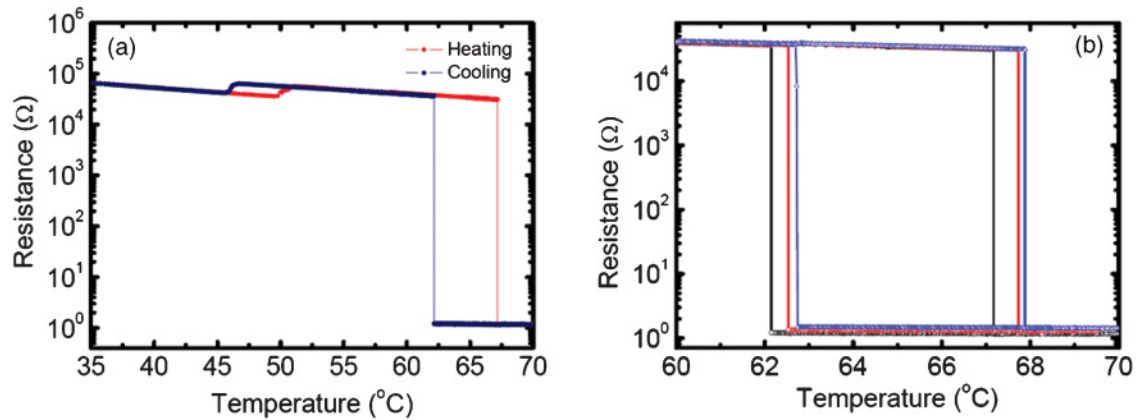


FIG. 1. (Color) (a) Resistance-temperature curve of a  $\text{VO}_2$  single crystal. The red and blue lines denote increasing and decreasing temperatures, respectively. (b) Thermal cycle dependence of MIT temperature at a fixed temperature ramp rate of  $0.1\text{ }^\circ\text{C}/\text{min}$ .

of almost 5 orders of magnitude. Interestingly, the onset temperature of the MIT exhibits run-to-run variation of up to  $\sim 1\text{ }^\circ\text{C}$  under a constant ramp rate,  $0.1\text{ }^\circ\text{C}/\text{min}$ . [Fig. 1(b)]. We attribute this to variable super-cooling (super-heating) effects caused by the kinetic barrier of the first-order phase transition.<sup>14</sup>

Because of the significant difference of the optical reflectivity of the metallic and insulating phases in  $\text{VO}_2$ , optical microscopy can be applied to monitor the presence and position of the sharp MIT phase boundary. Optical microscope images displayed in Fig. 2 clearly show the propagation of the MIT phase boundary as a function of time in both heating ( $T \sim 66.8\text{ }^\circ\text{C}$ ) and cooling ( $T \sim 61.2\text{ }^\circ\text{C}$ ) conditions (temperature ramp rate =  $1.0\text{ }^\circ\text{C}/\text{min}$ ). Figure 2 covers a time interval of  $\sim 1$  sec. No significant temperature variation was recorded in this time span. The dark and bright areas represent the metallic and insulating states of  $\text{VO}_2$ , respectively. Propagation speed was measured with a uniform sample temperature at the

fixed-ramp rate. The propagation speed of the phase boundary during the heating process ( $0.46 \pm 0.04$  mm/s) is about 2.5 times as fast as the one during cooling ( $0.19 \pm 0.02$ ) mm/s. The magnitude of the phase boundary speed in our  $\text{VO}_2$  sample is in good agreement with those in a sample of multiple phase boundaries.<sup>15</sup> The difference in speed between the two directions is possibly due to the different thermal conductivity between the metallic and insulating phase.<sup>16</sup> As shown in Fig. 2, the phase boundary is observed to move parallel to the elongated side of the crystal, which in turn corresponds to the rutile  $c$  axis. From the optical microscope images in Fig. 2 it can be seen that the metallic (dark—reflecting) and insulating (light—transparent) states are separated by a sharp interfacial boundary. However, the identity of the structural phases responsible for the dark and light contrasts is not evident from optical imaging. We therefore carried out an experiment in which both resistance and  $\mu$ -XRD patterns of  $\text{VO}_2$  single crystals were measured simultaneously as a function of temperature on beamline 12.3.2 at the Advanced Light Source of the Lawrence Berkeley National Laboratory.<sup>17</sup>

In the  $\mu$ -XRD experiment we collected Laue diffraction, i.e., white-beam single-crystal diffraction, exposures along the horizontal direction (i.e., along the rutile  $c$  axis) with a step size of  $10\text{ }\mu\text{m}$  between images and using a nominal x-ray beam size of about  $1\text{ }\mu\text{m}$ . These line scans of  $\mu$ -XRD provide critical spatial mapping of the SPT across the sample area with micron-scale resolution. Figure 3 displays the simultaneously recorded resistance [Fig. 3(a)] and Laue diffraction patterns [Fig. 3(b)] during the temperature ramp. Sections of Laue diffraction images are shown in Fig. 3(b) for easy comparison of the three phases (M1, M2, and R) of  $\text{VO}_2$ . The lattice parameters of each structure were retrieved from the literature in order to fit the Laue diffraction patterns.<sup>18</sup> Diffraction spots marked “S” arise from the sapphire wafer used for sample mounting. Figure 3(b) shows that our  $\text{VO}_2$  sample consists of pure monoclinic insulating M2 phase at  $25\text{ }^\circ\text{C}$  (I). The M2 phase remained present up to  $50\text{ }^\circ\text{C}$  (II). The temperature of  $52\text{ }^\circ\text{C}$  marks the onset of the coexistence of the M1 and M2 phases. Above  $52.5\text{ }^\circ\text{C}$  (IV) only the pure monoclinic insulating M1 phase was

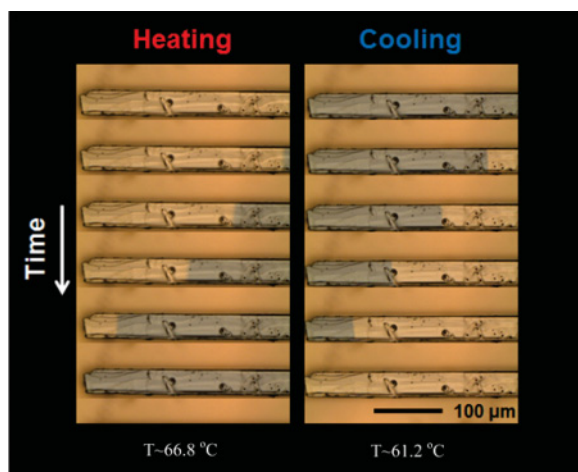


FIG. 2. (Color) Images of optical microscope during the onset of MIT near  $T = 66.8\text{ }^\circ\text{C}$  (heating) and  $T = 61.2\text{ }^\circ\text{C}$  (cooling) taken within  $\sim 1$  sec, respectively. The boundary of metal-insulator phase propagates along the rutile  $c$  axis of a  $\text{VO}_2$  crystal.

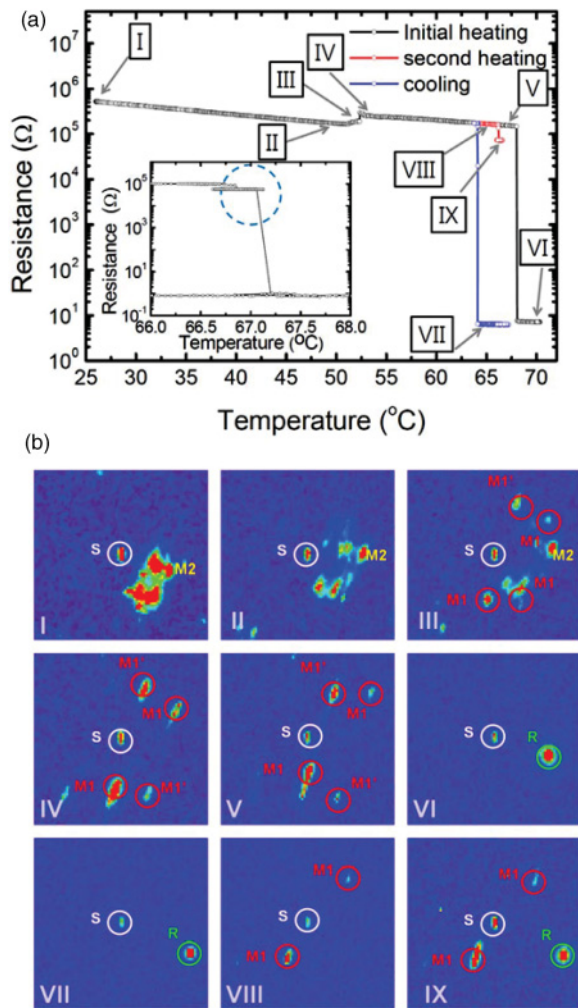


FIG. 3. (Color) Laue patterns from x-ray diffraction as a function of temperature. (a) and (b) At  $T = 25^{\circ}\text{C}$  (I), the insulating M2 phase is present. As the temperature increases to  $50\sim 52.5^{\circ}\text{C}$  (II, III, and IV), the coexistence of phases M1 and M2 can be seen. The M1 phase remains up to the MIT, which occurs at  $68^{\circ}\text{C}$  (V). The R phase shows immediately after the MIT at  $68.2^{\circ}\text{C}$  (VI). After undergoing a MIT in the cooling process (VII and VIII), the coexistence of M1 and R phases are shown when the temperature is set to  $66.2^{\circ}\text{C}$ , accompanied by a decrease in resistivity. Letter S inside the figures represents diffraction peak from the sapphire wafer used for sample mounting. (Inset) Spontaneous MIT of  $\text{VO}_2$  was stopped in the middle of the transition. The state remained quasistable with temperature variation ( $\pm 0.3^{\circ}\text{C}$ ) for 30 minutes. Then this quasistable insulating state made a transition to metallic state. M1 and M1' denote two twin domains of the M1 phase.

observed, and this M1 phase remained stable up to  $68.0^{\circ}\text{C}$  (V), right before the onset of the MIT. Immediately after passing  $68.0^{\circ}\text{C}$  (VI) the resistance drops  $\sim 5$  orders of magnitude, and only the pure tetragonal metallic R phase is observed in the Laue pattern. We associate this with the first-order MIT of  $\text{VO}_2$ . After the sample reached  $70^{\circ}\text{C}$  the temperature was lowered to  $65^{\circ}\text{C}$  (VII) at which point it remained in the metallic R phase. When the sample was cooled below  $64^{\circ}\text{C}$ , the insulating M1 phase reappeared. After identifying the transition temperature upon cooling at  $64^{\circ}\text{C}$ , the sample was

slowly heated back to  $66^{\circ}\text{C}$  (VIII), at a ramp rate of roughly  $0.3^{\circ}\text{C}/\text{min}$ . When the sample temperature reached  $66.2^{\circ}\text{C}$  (IX) there was a sharp boundary between the M1 and R phases with the crystal spatially divided into M1 and R phase, and only the Laue pattern at the boundary exhibited both monoclinic M1 and tetragonal metallic R phases, as shown in IX of Fig. 3(b). Simultaneously, the sample resistance was reduced by half. After observing both M1 and R phases at  $66.2^{\circ}\text{C}$ , the temperature was increased further to  $66.6^{\circ}\text{C}$ . Interestingly, the sample resistance remained unchanged and the coexistence of M1 and R phases persisted. This intermediate stage can be understood as a quasistable state of MIT, i.e., the SPT is completed only half way and the resistance is also reduced to half. Since the MIT occurs instantaneously at statistically varying transition temperatures, it is not easy to achieve this intermediate stage in a routine manner. A similar intermediate stage of MIT has been reproduced in additional resistance measurements [shown in inset of Fig. 3(a)]. Considering the statistical behavior of critical temperatures of the MIT in our previous laboratory measurements, shown in Fig. 1, the point IX ( $66.2^{\circ}\text{C}$ ) is the critical temperature for MIT in the present measurement. Clearly the position IX of Fig. 3, i.e., the onset of the MIT, represents an abrupt spatial boundary between coexisting metallic R and insulating M1 phases, and this is consistent with what is shown in Fig. 2, where an abrupt boundary between metallic and insulating phases is found. Also, the Laue pattern at the position IX implies that there is no other structural phase except M1 and R phases at the onset of MIT. In a recent report of Corr *et al.*, no distinct structural phase other than M1 and R at MIT is observed with x-ray total scattering,<sup>19</sup> which is identical to what we report here in IX of Fig. 3.

In the percolative pictures MIT occurs when the different nanoscale domains of metallic and structural phases are connected, creating a continuous path for electrons to travel from one domain to the other. In addition near the MIT temperature the mixtures of M1 and R phases should exist throughout the entire sample area if the percolation prevails. On the other hand our experimental results show only pure M1 and R phases spatially separated at the MIT, suggesting a nonpercolative behavior. At position IX of Fig. 3, the mixed state of R and M1 appears only in a single exposure, where the beam ( $\sim 1\ \mu\text{m}^2$ ) is directed onto the single boundary between M1 and R. This nonpercolative nature of our results is opposite to what has been reported previously.<sup>6-8</sup> In Ref. 6 nanopuddles, i.e., the mixed states composed of both metallic (R) and insulating (M1) phases, are observed and interpreted as signatures of percolation mechanism. However, our results, position IX in Fig. 3(b), does not show any indication for such a nanopuddle state. Our works suggest that the microscopic origin of MIT in  $\text{VO}_2$  may differ between high-quality single-crystal samples and thin film samples. Our results are reproduced on single-phase bulk  $\text{VO}_2$  crystals but look different on thin films.<sup>20</sup> Whether this gap can be bridged by changing sample related parameters, such as degrees of strain or defect, is an open question and calls for further efforts both in theory and experiment. Recently, Rini *et al.*<sup>21</sup> reported that the optical switching properties of polycrystalline  $\text{VO}_2$ -thin films are significantly different from those of high quality  $\text{VO}_2$  single crystals. It will be very interesting to revisit many important previous findings with our  $\text{VO}_2$  single



crystals, for example, the presence of electronic and crystalline phase transitions near the MIT temperature,<sup>6,7</sup> hole-driven MIT phenomena,<sup>22</sup> and time-resolved photo excitation.<sup>23</sup>

In summary we studied the characteristics of the phase boundary of MIT propagating along the *c* axis of a VO<sub>2</sub> single-crystal sample. With  $\mu$ -XRD and optical microscope, the coexistence of monoclinic M1 and rutile R phases is observed with a sharp spatial boundary at the onset of MIT. Our study reveals strong evidence that the MIT in a VO<sub>2</sub> single crystal occurs in a nonpercolative way.

This work was supported by Advanced Nano Products Co., Ltd. B. S. M would like to thank the support by the Korea Research Foundation (KRF) grant funded by the Korean government (MEST) (No. 2009-0068720). The Advanced Light Source is supported by the Director, Office of Science, Office of Basic Energy Sciences, Materials Science Division, of the US Department of Energy under Contract No. DE-AC02-05CH11231 at LBNL. The microdiffraction program at the ALS on BL 12.3.2 was made possible by NSF Grant No. 0416243.

\*tesl@yonsei.ac.kr

- <sup>1</sup>J. Morin, *Phys. Rev. Lett.* **3**, 34 (1959).
- <sup>2</sup>N. F. Mott, *Rev. Mod. Phys.* **40**, 677 (1968).
- <sup>3</sup>A. Zylbersztejn and N. F. Mott, *Phys. Rev. B* **11**, 4383 (1975).
- <sup>4</sup>R. M. Wentzcovitch, W. W. Schulz, and P. B. Allen, *Phys. Rev. Lett.* **72**, 3389 (1994).
- <sup>5</sup>J. B. Goodenough, *J. Solid State Chem.* **3**, 490 (1971).
- <sup>6</sup>M. Qazilbash, M. Brehm, Byung-Gyu Chae, P.-C. Ho, G. O. Andreev, Bong-Jun Kim, Sun Jin Yun, A. V. Balatsky, M. B. Maple, F. Keilmann, Hyun-Tak Kim, and D. N. Basov, *Science* **318**, 1750 (2007).
- <sup>7</sup>M. Qazilbash, A. Tripathi, A. A. Schafgans, Bong-Jun Kim, Hyun-Tak Kim, Zhonghou Cai, M. V. Holt, J. M. Maser, F. Keilmann, O. G. Shpyrko, and D. N. Basov, *Phys. Rev. B* **83**, 165108 (2011).
- <sup>8</sup>Y. J. Chang, J. S. Yang, Y. S. Kim, D. H. Kim, T. W. Noh, D.-W. Kim, E. Oh, B. Kahng, and J.-S. Chung, *Phys. Rev. B* **76**, 075118 (2007).
- <sup>9</sup>D. Stroud, *Phys. Rev. B* **12**, 3368 (1975).
- <sup>10</sup>K. Lai, M. Nakamura, W. Kundhikanjana, M. Kawasaki, Y. Tokura, M. A. Kelly, and Z.-X. Chen, *Science* **329**, 190 (2010).
- <sup>11</sup>M. Fäth, S. Freisem, A. A. Menovsky, Y. Tomioka, J. Aarts, and J. A. Mydosh, *Science* **285**, 1540 (1999).
- <sup>12</sup>A. Sharoni, J. G. Ramirez, and I. K. Schuller, *Phys. Rev. Lett.* **101**, 026404 (2008).
- <sup>13</sup>B. S. Mun, Kai Chen, Youngchul Leem, Catherine Dejoie, Nobumichi Tamura, Martin Kunz, Zhi Liu, Michael E. Grass, Changwoo Park, Joonseok Yoon, Y. Yvette Lee, and Honglyoul Ju, *Phys. Status Solidi RRL* **5**, 107 (2011).
- <sup>14</sup>J. Wei, Z. Wang, W. Chen, and D. H. Cobden, *Nature Nanotechnology*, **4**, 420 (2009).
- <sup>15</sup>B. Fisher, *J. Phys. C: Solid State Phys.* **9**, 1201 (1976).
- <sup>16</sup>D. Oh, C. Ko, S. Ramanathan, and D. G. Cahill, *Appl. Phys. Lett.* **96**, 151906 (2010).
- <sup>17</sup>M. Kunz, N. Tamura, K. Chen, A. A. MacDowell, R. S. Celestre, M. M. Church, S. Fakra, E. E. Domning, J. M. Glossinger, J. L. Kirschman, G. Y. Morrison, D. W. Plate, B. V. Smith, T. Warwick, V. V. Yashchuk, H. A. Padmore, and E. Ustundag, *Rev. Sci. Instrum.* **80**, 035108 (2009).
- <sup>18</sup>J. Cao, Y. Gu, W. Fan, L. Q. Chen, D. F. Ogletree, K. Chen, N. Tamura, M. Kunz, C. Barrett, J. Seidel, and J. Wu, *Nano Lett.*, **10**, 2667 (2010).
- <sup>19</sup>S. A. Corr, D. P. Shoemaker, B. C. Melot, and R. Seshadri, *Phys. Rev. Lett.* **105**, 056404 (2010).
- <sup>20</sup>B. S. Mun, J. Yoon, K. Chen, C. Dejoie, N. Tamura, M. Kunz, Z. Liu, M. E. Grass, S.-K. Mo, C. Park, and H. Ju (in preparation).
- <sup>21</sup>M. Rini, Z. Hao, R. W. Schoenlein, C. Giannetti, F. Parmigiani, S. Fourmaux, J. C. Kieffer, A. Fujimori, M. Onoda, S. Wall, and A. Cavalleri, *Appl. Phys. Lett.* **92**, 181904 (2008).
- <sup>22</sup>H.-T. Kim, Yong Wook Lee, Bong-Jun Kim, Byung-Gyu Chae, Sun Jin Yun, Kwang-Yong Kang, Kang-Jeon Han, Ki-Ju Yee, and Yong-Sik Lim, *Phys. Rev. Lett.* **97**, 266401 (2006).
- <sup>23</sup>A. Cavalleri, Cs. Tóth, C. W. Siders, J. A. Squier, F. Ráksi, P. Forget, and J. C. Kieffer, *Phys. Rev. Lett.* **87**, 237401 (2001).